The analysis of distributions of effective strain and flow stress in longitudinal sections of cold backward extruded copper cans for different punch-face shapes

Tomasz Miłek[1,*]

[1]Kielce University of Technology, Faculty of Mechatronics and Mechanical Engineering, Department of Applied Computer Science and Armament Engineering, al. Tysiąclecia Państwa Polskiego 7, 25-314 Kielce, Poland, UE

Abstract. The paper presents computer modelling results of researches on cold backward extrusion of copper cans. The calculations were carried out using the commercial code QFORM-2D, based on the Finite Element Method (FEM). The simulation of cold backward extrusion process was performed for different punch-face shapes (flat; flat and conical with conical angle 90^0 and 150^0; as well as concave). On the basis of obtained results, the analysis of distributions of effective strain and flow stress in longitudinal sections of cold backward extruded copper cans was conducted.

1 Introduction

The process of backward extrusion of cans still plays an important role in the manufacturing industries [1]. Copper cans are traditionally produced in multi-stage deep drawing processes which, however, have some drawbacks, namely the design cost, material waste and inconsistent wall thickness [2,3]. Backward extrusion could be considered an alternative manufacturing process to produce cans [4]. When compared with other manufacturing processes, backward extrusion offers many advantages, including lower material consumption, higher dimensional accuracy and surface quality, adequate mechanical and microstructural properties and reduction or complete elimination of machining. Products after extrusion have better mechanical properties than those of the original material due to favourable grain flow [5-7]. Although backward extrusion has significant capabilities in production, it also shows some limitations. The unsteady deformation zone, which causes different strain distribution through the extruded part, is one of the problems [5].

The backward extrusion process, in which metal flows in the opposite direction to that of the punch movement, is relatively more energetically efficient. In the process, friction is considerably reduced, because the friction along the chamber walls does not need to be overcome. The material coming through the orifice formed by the punch land and the die wall undergoes no strain after this point. The remaining volume between the punch and the die bottom (or the ejector) is only partly located in the deformation zone. Depending upon the geometrical and friction conditions, a dome-shaped rigid plastic zone is formed in this region. The factors that affect the zone mentioned above include the can bottom thickness and the reduction in the area [2].

The deformation ratios of material in the literature [2,3,8] was defined as relative: strain of can bottom thickness ε_h, reduction in the area ε_A and equivalent strain ε. The strain ε_h, is calculated according to the following formula [2,3]:

$$\varepsilon_h = \frac{\Delta h}{h_o} = \frac{h_0 - h_1}{h_0} \tag{1}$$

where:
Δh – the punch displacement in mm,
h_0 – billet height in mm,
h_1 – thickness of cup bottom in mm,
The reduction in the area ε_A can be estimated from the relationship given below [2,3]:

$$\varepsilon_A = \frac{A_0 - A_s}{A_0} = \frac{d_0^2 - d_s^2}{d_0^2} \tag{2}$$

where:
A_0 – cross sectional area of the billet in mm^2,
A_1 - cross sectional area of the die stamping in mm^2,
d_0 – diameter of billet in mm,
d_s – diameter of punch in mm,

The unit operation of work of plastic deformation in industrial practice is determined by the homogeneous equivalent strain ε. It is given by a formula [8]:

$$\varepsilon = \ln \frac{A_0}{A_1} \tag{3}$$

1.1 State of the art

Cold backward extrusion of circular-shaped parts made from copper and aluminium and the design of the tooling have been reported in some studies [1,4,5,7,9-20]. Those covered both experimental and computer modelling investigations.

* Corresponding author: tmatm@tu.kielce.pl

Lee and Kwan [9] proposed a kinematically modified admissible velocity field for the backward extrusion of internally circular-shaped tubes from arbitrarily shaped billets. From the proposed velocity field, the upper-bound extrusion load and average extruded height for regular polygonal-shaped billets were determined with respect to the chosen parameters.

Zasadziński [10] evaluated the usefulness of different methods for continuous extrusion of aluminium and its alloys, based on the analysis of active friction forces possible to achieve in these methods. The Linex, Extrolling, Conform processes, as well as two methods proposed by the author were analysed.

Y.H. Kim and Park [11] studied backward extrusion process with low die rotation. The objective of investigations was to address problems related to conventional backward extrusion process, namely the necessity of using a large forming machine, the difficulty in selecting the die material due to high surface pressure, costs related to the reduction in noise and vibration generated from the forming machine, and others. They analysed experimental results for torsional and conventional backward extrusions. Results were compared using two methods, i.e. upper bound technique for computing the velocity field, and FEM simulation with DEFORM-3D.

Thomas [12] conducted a series of investigations into cold backward extrusion of cans for copper before and after heat treatment. He analysed the experimental change of the force for copper cans at the reduction in area ε_A=0,360-0,639.

Żmudzki A. et al. [13] presented numerical (FEM) and experimental results of the analysis of tests, which were performed to determine the friction coefficient in two types of metal forming processes (ring compression and combined forward-backward extrusion). Experiments were performed for copper deformed at room temperature. Żmudzki A. et al. demonstrated that friction coefficient calculated from the ring compression tests was slightly lower that determined from the direct-indirect extrusion test.

In their study, Shatermashhadi V. et al. [1], proposed a method of backward extrusion using small diameter billet. Their die setup consisted of three major components, namely the fix-punch, the moveable punch and the matrix. They demonstrated that the load was reduced to about less than a quarter when compared with the conventional backward extrusion process. Shatermashhadi V. et al. also conducted numerical investigations, in which the DEFORM 3D software was used for FE simulations. In their another work [7], they discussed the applications of the modified process to commercially pure aluminium.

Kim et al. [4] evaluated the effects of lubricants in backward extrusion of a rectangular aluminium case with large aspect ratio. The analysis of backward extrusion of a rectangular aluminium box for electrical battery casing was performed using MSC SuperForge, commercial finite volume software. The numerical analysis showed clearly that a friction factor of 0.2 yields an optimal forming shape, which was independently confirmed by experimental results.

Farhoumand and Ebrahimi [5] examined the effects of geometrical parameters including die corner radius and gap height, and of the process conditions, such as friction, on the radial-backward extrusion process.

In Wang et al. [14], recent developments in the friction testing techniques for aluminium extrusion processes were discussed and detailed comparisons of these techniques were made.

The most papers are concerned with the analysis on the forming of copper in micro-backward can extrusion process [15-20]. Ch. Chang et al. [15] discussed the effects of temperature and grain size on the deformation, dimension variation, and change of microstructure of copper from combined backward and forward extrusion at the micro scale. They conducted a series of investigations into extrusion of copper micro cups with 0.1 mm thickness. Three forming temperatures: 25, 200 and 400 ºC, were considered in the micro extrusion experiments. Their studies show that the grain refinement improves material flow and thus lead to a better die filling with less variation in the rim height and wall thickness of the cup portion of the extruded part at relatively lower forming temperature.

Wang et al. [16] demonstrated that forming process of dispersion strengthened copper welding electrode consists of a forward extrusion and a backward extrusion. They analysed the characteristics of metal flow and the effect of different friction factors. Wang et al. [16] carried out the simulation of the upsetting-extruding process using Deform-2D finite element analysis software.

Geisdorfer et al. [17] investigated a possibility of using an ultrafine grained copper for micro-extrusion. The microforming process of backward extrusion was carried out at room temperature using half cylindrical billets. The extrusion force, grain flow, shape representation and surface quality of the extruded micro-components were compared.

Chan et al. [18] studied a size effect in micro-extrusion process of pure copper. The size effect on material deformation behaviours was characterised by grain size, part feature size, forming material size and interfacial condition. Chan et al. [18] performed research on micro-forward, backward, combined forward rod-backward can and double cup extrusions.

Bazaz et al. [19] evaluated the microstructure evolution of a pure copper processed by accumulative back extrusion (ABE) method at room temperature. The analysis of microstructure and hardness showed outstanding homogeneity improvement throughout the workpieces.

L. Yi et al. [20] proposed theoretical model to predict the backward extrusion force of copper-chromium alloy based on Projection Pursuit Regression (PPR).

1.2 The aim of investigations

The paper presents computer modelling (FEM) results of investigations on cold backward extrusion of copper cans. The different punch-face shapes were used for cold extrusion (flat; flat and conical with conical angle 90^0

and 150^0 and concave). Based on obtained results at relative strains ε_h=0,69 and ε_A= 0.67 and ε= 1.1, the analysis of distributions of effective strain and flow stress in longitudinal sections of cold backward extruded copper cans was conducted. Pure copper was selected as the testing material in these investigations due to its excellent formability and wide applications in industry.

2 Models and assumptions in numerical modelling with QFORM-2D

Computer modelling of metal forming processes is nowadays widely used for optimisation and shape prediction of newly designed parts during their manufacturing. At present there are many FEM systems to numerically investigate metal forming processes. Programs related to issues of forging and extrusion include: QForm MSC Superform, Deform, Forge, MSC Marc. QForm-2D/3D (Quantor-Form Ltd., Russia) uses the flow formulation for material behaviour. The estimation of the QForm simulation results was carried out in several works [21-24]. The analysis of these papers shows the good compatibility between the results of numerical simulation and experimental data.
Calculations of metal flow and study distributions of effective strain, flow stress and changes in loading were carried out with commercial code QFORM2D based on Finite Element Method (FEM).
The extruded material was incompressible rigid-plastic continuum and elastic deformations were neglected. The system of governing equations included the following [22,25]:

- equilibrium equations
$$\sigma_{ij,j} = 0 \tag{4}$$
- compatibility conditions
$$\dot{\varepsilon}_{ij} = \frac{1}{2}(v_{i,j} + v_{j,i}) \tag{5}$$
- constitutive equations
$$\sigma'_{ij} = \frac{2\bar{\sigma}}{3\dot{\bar{\varepsilon}}}\dot{\varepsilon}_{ij} \tag{6}$$
- incompressibility equation
$$v_{i,i} = 0 \tag{7}$$
- expression for flow stress
$$\bar{\sigma} = \bar{\sigma}(\bar{\varepsilon}, \dot{\bar{\varepsilon}}, T) \tag{8}$$

where σ_{ij} and $\dot{\varepsilon}_{ij}$ – components of stress and strain-rate tensors, v_i – velocity components, σ'_{ij} – deviatoric stress tensor, $\bar{\sigma}, \bar{\varepsilon}, \dot{\bar{\varepsilon}}$ – effective stress, strain and strain-rate, respectively, T – temperature.

In Eqs 4-8, summation convention was used. The prime denoted a derivative with respect to the axis following it. The indexes i and j for two-dimensional problems varied from 1 to 2, and repeated subscript represented summation.

The friction model proposed by Levanov et. al [22,25] was used for the contact region of workpiece surface. Eq. (9) could be considered as a combination of the constant friction model and the Coulomb friction model. The formula combined the advantages of both models [22,25]:

$$F_t = m\frac{\bar{\sigma}}{3}(1 - \exp(-1{,}25\frac{\sigma_n}{\bar{\sigma}}) \tag{9}$$

where m was the friction factor, σ_n was the normal contact pressure.

The flow stress characteristics were given as a function of the strain rate:

$$\bar{\sigma} = C\bar{\varepsilon}^n \tag{10}$$

Based on literature data [26] Eq. (10) was adopted for numerical modelling of cold backward extrusion of copper cans:

$$\bar{\sigma} = 420\bar{\varepsilon}^{0.3} \tag{11}$$

The investigations into backward extrusion involved the use of circular sectioned copper segments of rods with diameter d_0 = 24.5 mm and height h_0 = 16 mm (h_0/d_0=0.65). A tool for backward extrusion was equipped with replaceable punches with different punch shapes and constant diameter d_s= 20mm (Fig. 1). Initial workpiece and tools temperatures were 20^0C and 10^0C, respectively.

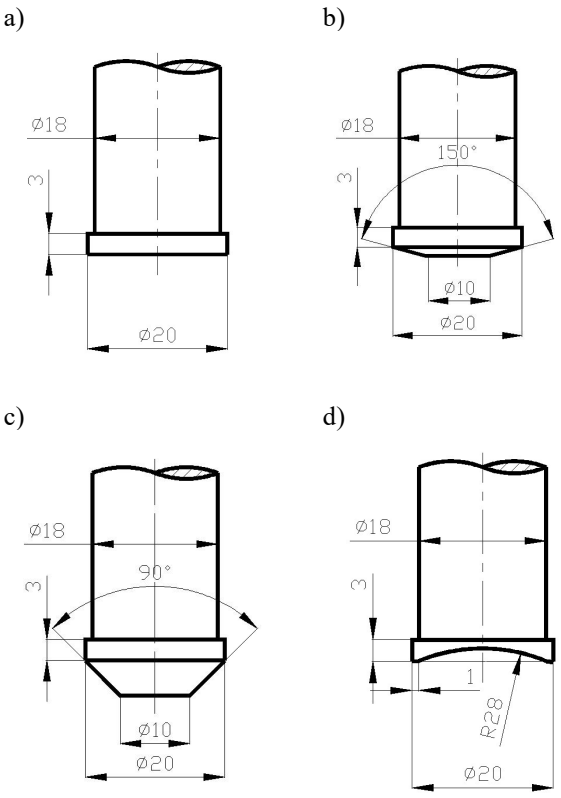

Fig. 1. The different punch-face shapes used in experiment and modelling of cold backward extrusion of copper cans: a) flat; b) flat and conical with a conical angle 150^0; c) flat and conical with a conical angle 90^0 d) concave.

3 Results and analysis

The numerical investigations produced copper cans in cold backward extrusion with strain of can bottom thickness ε_h=0.69 and reduction of the area ε_A= 0.67 and homogeneous equivalent strain ε=1.1 for different punch-face shapes (flat; flat and conical with conical angle 90^0 and 150^0 and concave). Results of the simulation process showed that the model of boundary conditions, presented in previous chapter, proved adequate. To analyse metal flow in the computer program, the flow lines were imposed. They formed a grid that made it possible to view the displacement and distortion of the metal selected volumes in deformations. In the simulation, ten inner flow lines along the OX and OY axes were assumed. Numerically calculated last stages of backward extrusion for different punch-face shapes are presented in the Fig. 2.

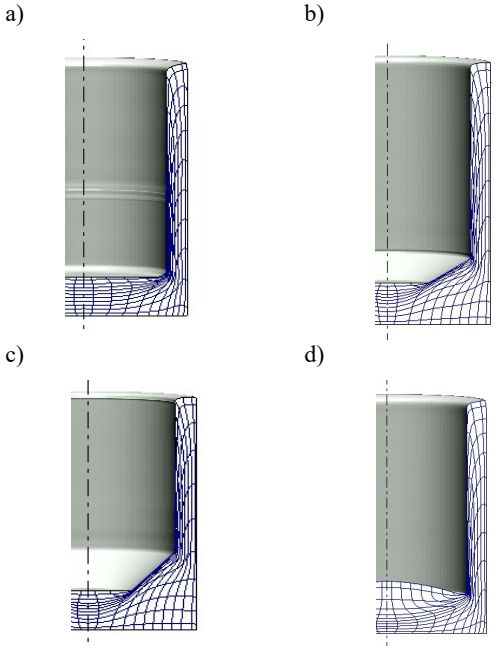

Fig. 2. Numerically calculated last stages a.- d. (which corresponded to equivalent strain ε=1.1 and ε_A= 0,67) of backward extrusion of copper can for different punch shapes: a) flat, b) flat and conical flat with conical angle 150^0, c) flat and conical with conical angle 90^0, d) concave.

The analysis of the flow lines confirmed the literature conclusions [2,3,8,23,27] concerning the occurrence of characteristic areas in the cross-section of extruded stampings at flat punch-face shape. The flow lines below the punch exhibit a curvature about the axis and the streamlines are curved toward the outside [3]. There are four zones of deformation in the cross-section of cans [2,3,8,23,27]. The lowest hardening area is located outside of the bottom part and the upper part of can. The intermediate area includes the inner part of the bottom and the zone adjacent to the outer wall of the product. The strongest hardening area occurs at the inner surface of the can wall. The described deformation zones have also been observed in investigations of cold backward extrusion of copper cans for different punch-face shapes (Fig. 2a-d). The most deformed flow lines were observed in longitudinal sections of cold backward extruded copper cans at flat punch-face and flat and conical punch-face shapes with conical angle 90^0 (Fig. 2a and Fig. 2b).

The analysis of the process was conducted based on results of numerically computed effective strain and flow stress distributions at intersections of backward extruded die stampings, too (Fig. 3 and Fig. 4).

Based on the analysis of numerically calculated effective strain distribution (shown in the Fig. 3) at the intersection of backward extruded cans made from copper, it can be stated that in the different stages of the modelling, the maximum effective strain values were found in the die stamping inner wall forming and area of the inner radii of the bottom transition to the wall. The maximum value of the effective strain was found in the last stage of simulation of cold backward extrusion for copper can extruded with concave punch shape. It occurred in inner walls and reached the value of 5.652 (Fig. 3d). In all stages of simulation of cold backward extrusion of copper cans for concave punch shape considered values of the effective strain were higher than values obtained for extruded die stampings by using other punch shapes (flat; flat and conical with conical angle 90^0 and 150^0 and concave, respectively). In cold backward extrusion of copper cans with strain of can bottom thickness ε_h = 0.69 and reduction of the area ε_A = 0.67 and homogeneous equivalent strain ε=1.1, maximum value of the effective strain obtained in longitudinal section extruded die stamping for flat and conical punch-face shape with conical angle 150^0 (Fig. 3b) did not differ much from maximum value of the effective strain for can formed at conical punch-face shape (Fig. 3c) with conical angle 90^0 (3.919 and 3.870, respectively). The maximum value of the effective strain obtained for copper can with flat punch-face shape (3.306) was smaller by approx. 41 % than the value obtained for die stamping with concave punch-face shape (Fig. 3d). The lowest values of effective strain occurred slightly outside the projection of the punch edges on the bottom surface for all types of punches (Fig. 3a-d).

Numerically obtained flow stress distributions in longitudinal sections of cold backward extruded copper cans for different punch shape are presented in the Fig. 4a-d. No significant differences were found while analysing the maximum values of flow stress for cold backward extrusion of copper cans for different punch-face shape. The highest value of the flow stress was noted in last stages of simulation for all punch shapes. It amounted to 420MPa (Fig. 4a-d). The main differences were observed in changes of distribution of flow stress in intersection of cold backward extruded cans. The area of maximum flow stresses occurred in inner walls of copper cans in all cases of punch shapes (Fig. 4a-d) and in the bottom of die stampings for backward extrusion at flat punch-face (Fig. 4a). The zone of relative lower flow stresses was observed outside of the bottom part (corners of the die) for extrusion at flat and conical punch-face shapes with conical angle 90^0 and 150^0 (Fig. 4b and Fig. 4c). Besides, it was located the inner part of the bottom for die stamping with concave punch-face shape (Fig. 4d).

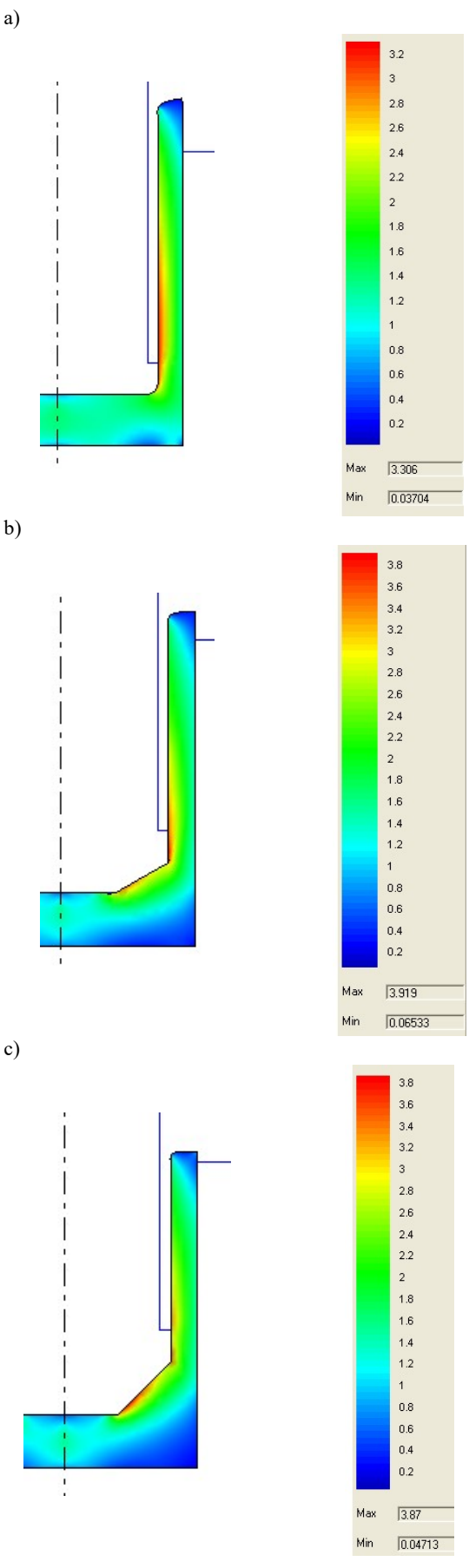

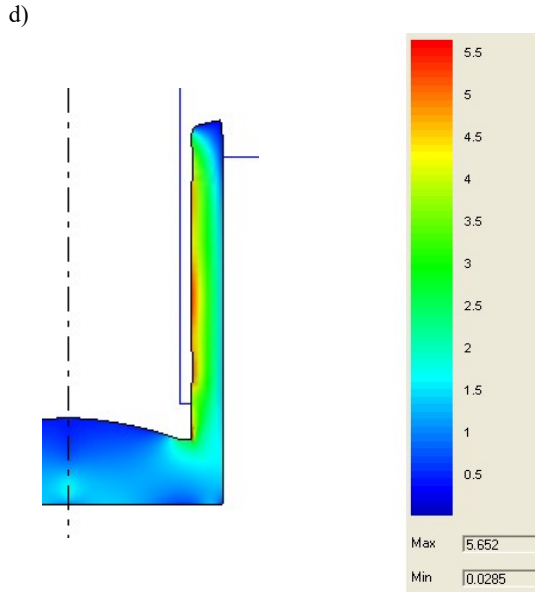

Fig. 3. Numerically computed effective strain distribution at the intersection of backward extruded can for the last stage of computer modelling ($\varepsilon_h = 0.69$; $\varepsilon_A = 0.67$; $\varepsilon = 1.1$) and for different punch shapes: a) flat, b) flat and conical flat with conical angle 150^0, c) flat and conical with conical angle 90^0, d) concave

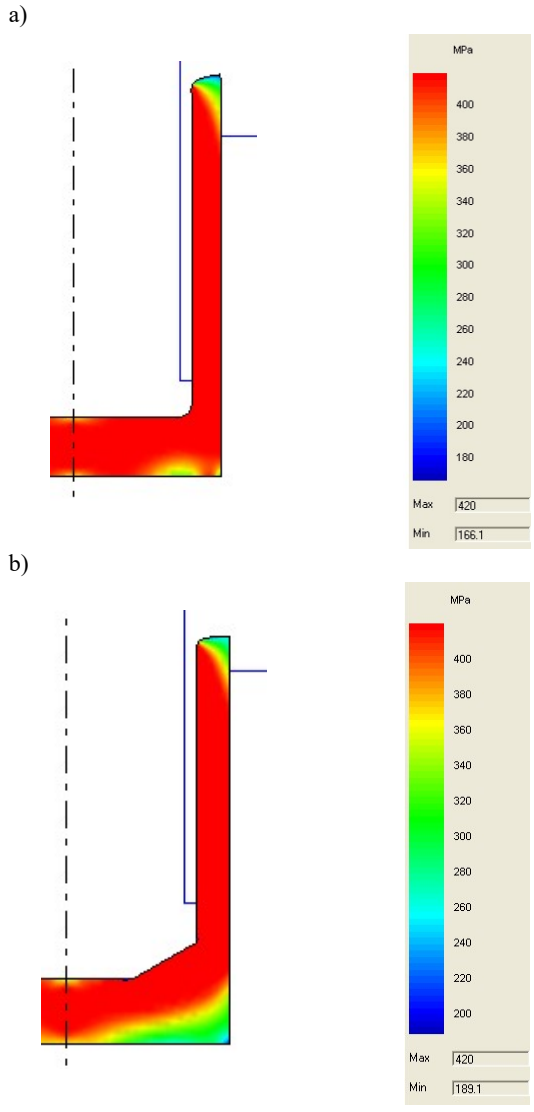

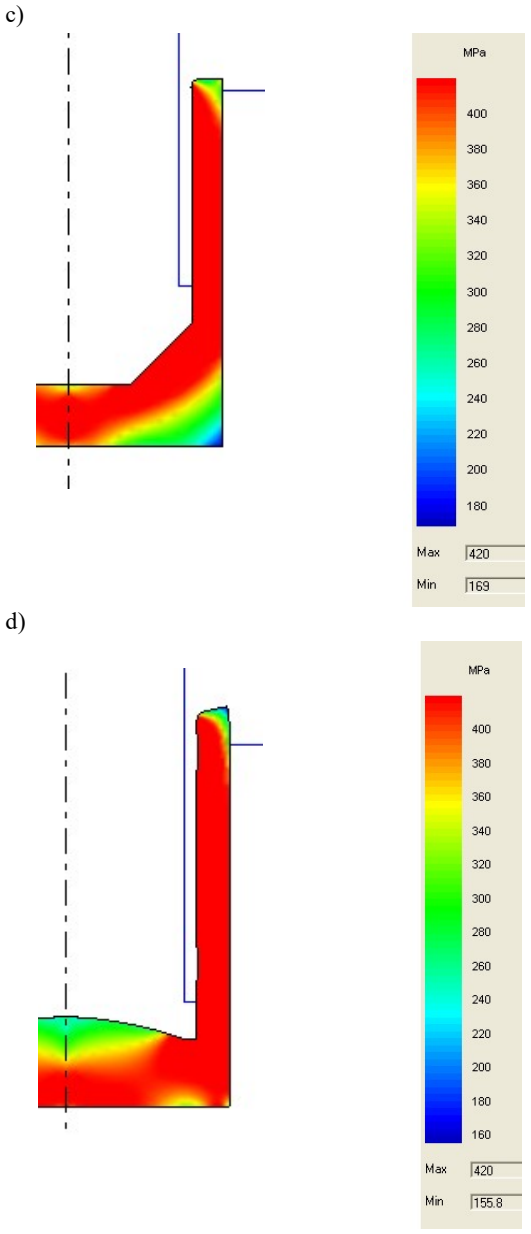

Fig. 4. Numerically computed flow stress distribution at the intersection of backward extruded can for the last stage of computer modelling ($\varepsilon_h = 0.69$; $\varepsilon_A = 0.67$; $\varepsilon = 1.1$) and for different punch shapes: a) flat, b) flat and conical flat with conical angle 150^0, c) flat and conical with conical angle 90^0, d) concave

Results of calculations of cold backward extrusion of copper cans process were validated against experimental data in terms of changes in forces for different punch shape. For the assumed maximum punch displacement Δh=11mm (which corresponded to the $\varepsilon_h = 0.69$; $\varepsilon_A = 0.67$; $\varepsilon = 1.1$) successful experimental tests were conducted (Fig. 5). The 2D FE models successfully described the backward extrusion of copper cans. Comparing changes in forces in cold backward extrusion for different punch shape, a conclusion that the load P_w increases with an increase in displacement Δh and strain of can bottom thickness $\varepsilon_{h\,can}$ [23].

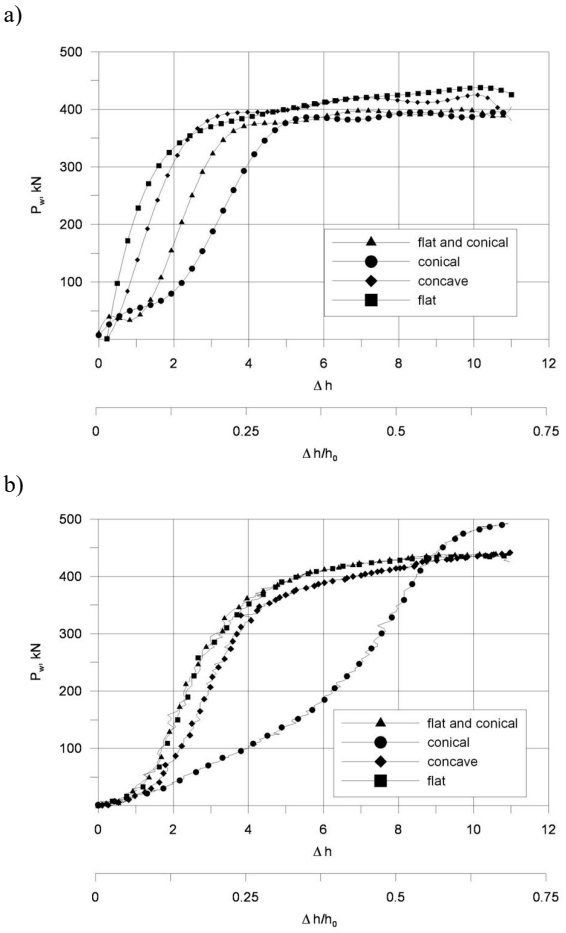

Fig. 5 The influence of punch shape on the cold backward extrusion force for copper cans at ε_A= 0,67 and ε= 1,1: a) numerical results, b) experimental investigations [23].

4 Summary

Although commercial package of QForm2D has been especially designed for numerical simulation of forging processes, the 2D FE model successfully described the backward extrusion of copper cans. It was possible to conduct cold backward extrusion of copper cans with strain of can bottom thickness ε_h=0.69 and reduction of area ε_A= 0.67 and homogeneous equivalent strain ε=1.1 for different punch-face shapes (flat; flat and conical with conical angle 90^0 and 150^0 and concave). It is confirmed by results of successfully performed computer modelling in these paper and experimental tests presented in previous author's studies [23]. The maximum value of the effective strain obtained for copper can with concave punch-face shape was higher by approx. 70 % than the value obtained for die stamping with flat punch-face shape. No significant differences were found while analysing the maximum values of flow stress for cold backward extrusion of copper cans with for different punch-face shape. The highest value of the flow stress was noted in last stages of simulation for all punch shapes.

References

1. V. Shatermashhadi, B. Manafi, K. Abrinia, G. Faraji, M. Sanei, Mater. Des. **62**, 361 (2014).
2. K. Lange, *Handbook of metal forming* (McGraw-Hill, Inc. USA,1985).
3. W. A. Golowin, A. N. Mitkin, A. G. Rieznikow, *Cold extrusion of metals* (WNT Warszawa, 1975).
4. S.H. Kim, S.W. Chung, S. Padmanaban, J. Mater. Process. Technol. **180**, 185 (2006).
5. A. Farhoumand, R. Ebrahimi, Mater. Des. **30,** 2152 (2009).
6. M. Plancak, M. Brameley, A. Osman F. J. Mater. Process. Technol. **34**, 465 (1992).
7. S.H. Hosseini, K. Abrinia, G. Faraji, Mater. Des. **65**, 521 (2015).
8. K. Kuczyński, E. Erbel, *Metal forming – lab* (Wyd. Polit. Warszaw., Poland, 1984).
9. R.S. Lee, C.T. Kwan, J. Mater. Process. Technol. **59**, 351 (1996).
10. J. Zasadziński, Rudy i Met. Nieżelazne **47**, 26 (2002).
11. Y.H. Kim, J.H. Park, J. Mater. Process. Technol. **143-144**, 735 (2003).
12. P. Thomas, Maint. Reliab. **2**, 63 (2003).
13. A. Żmudzki, R. Kuziak, M. Papaj, M. Pietrzyk, Obr. Plast. Met. **3**, 69 (2004).
14. L. Wang, J. Zhou, J. Duszczyk, L. Katgerman, Tribol. Int. **56**, 89 (2012).
15. Ch. Chang, J. Lin, Ch.-P. Siao, Steel Res. Int., spec. edit.: 14th Int. Conf. Met. Form. 467 (2012).
16. M. Wang, Y. Zhang, D. Huang, X. Liu, Trans. Nonferrous Met. Soc. China **17**, 449 (2007).
17. S. Geisdorfer, A. Rosochowski, L. Olejnik, U. Engel, M. Richert, Int. J. Mater. Form. **1**, 455 (2008).
18. W. Chan, M. W. Fu, B. Yang, Mater. Des. **32**, 3772 (2011).
19. B. Bazaz, A. Zarei-Hanzaki, S. Fatemi-Varzaneh, Material Science and Engineering A **559**, 595 (2013).
20. L. Yi, Y. Dong, M. Lin, L. Zhang, X. Wang, 2013 Int. Conf. on QR2MSE, 1181 (2013).
21. T. Miłek, B. Kowalik, B. Kuliński, Arch. Metall. Mater. **4**, 3043 (2015).
22. N. Biba, S. Stebunov, A. Vlasov, Steel Res. Int. **79**, 611 (2008).
23. T. Miłek, Mechanik **5/6**, 536 (2016).
24. T.Miłek, Int. Conf. Metal 2014, 285 (2014).
25. QFORM 2D/3D *Metal forming simulation program ver. 4.2. 2D simulation* (User's Guide, QuantorForm Ltd. 2007).
26. A. Mazurkiewicz, L. Kocur, *Metal forming – laboratory* (Wyd. Polit. Radom. 2001).
27. W. Muzykiewicz, A. Rękas, Rudy i Met. Nieżelazne **49**/10-11, 542 (2004).